Quasicrystallization of Vortices in Drift-Wave Turbulence

Nikolai Kukharkin, Steven A. Orszag, and Victor Yakhot
Fluid Dynamics Research Center, Princeton University, Princeton, New Jersey 08544
(Received 9 December 1994)

The formation and dynamics of coherent vortices in the Hasegawa-Mima two-dimensional model of drift-wave turbulence is studied numerically. The effect of "vortex shielding" due to the presence of a characteristic length scale (ion Larmor radius ρ_s) leads to important differences between self-organization in drift-wave and Navier-Stokes fluid turbulence. While it may not be surprising that a finite deformation radius leads to the formation of coherent vortices, we show here that it also results in the appearance of long-range order in the system, i.e., the formation of a vortical "quasicrystal."

PACS numbers: 47.27.Eq, 52.35.Ra

Conservation of enstrophy is the most important feature of two-dimensional (2D) hydrodynamics since it leads to the inverse energy cascade, i.e., creation of the large-scale energetic velocity fluctuations in the system where energy is introduced by an external source at some small scale $l_f \ll L$, L is the dimension of the flow. Simultaneously, small-scale structures, containing the dominant part of enstrophy, are formed due to the direct cascade. These two distinct dynamic processes lead to the self-organization, i.e., formation of coherent structures, such as isolated long-lived vortices in 2D Navier-Stokes (NS) turbulence [1–4]. It has been shown that these vortices appear in both driven and freely decaying turbulence, provided that the forcing and dissipation are not too strong. A necessary condition for the formation of strong coherent vortices is the accumulation of a significant amount of energy within regions of closed streamlines leading to the trapped trajectories of vorticity. Various mechanisms may lead to the formation of closed streamlines, the most typical of which is the small-scale roll up of sheared vortex filaments, stabilized by viscous smoothing. However, these small eddies are only *seed,* or *nuclei,* vortices and become coherent only if they trap enough energy to survive dissipation [5].

The above picture may hold in unbounded systems in which inversely cascaded quantities can expand to the ever larger scales. On the other hand, the spectra and dynamics of vortices can change significantly if there is a characteristic length scale which interferes with the inverse cascade. In Ref. [6] it is shown how isolated coherent 2D vortices can appear in driven Navier-Stokes turbulence after energy accumulates in the largest allowed scale, and therefore, under these conditions, intermittency is a finite-size effect. Energy pileup on a scale corresponding to the system size is only one example of a condensation process that can lead to the formation of coherent vortices, but it may be one relevant to atmospheric dynamics. Another scenario is investigated in [7], where the inverse energy cascade is artificially interrupted at a scale $l_0 = 1/k_T$. There the energy flux in wave-number space is $\Gamma(k) = \text{const} < 0$ at $k \geq k_T$ and $\Gamma(k) = 0$ at $k < k_T$, leading to energy accumulation in the mode $E(k_T)$. As a result, coherent vortices form a close to ideal crystal with the lattice constant l_0. The question arises whether this crystallization occurs in other inversely cascading systems which have "natural" rather than artificial length scales. One may expect that this kind of phenomenon is of general importance: Any dynamical mechanism leading to the decrease of otherwise constant energy flux ($\Gamma = \text{const}$ for $l \leq l_0$) can lead to energy pileup at scales $l \simeq l_0$ and creation of an ordered vortical phase.

In this Letter we will demonstrate that vortex "quasicrystals" do form for the Hasegawa-Mima (HM) equation [8]. This equation is an important paradigm for the description of drift-wave turbulence in magnetically confined plasmas (e.g., tokamaks) and has a structure identical to that of the Charney equation, describing geostrophic motions in planetary atmospheres [9,10]. In nondimensional form, the driven-damped Hasegawa-Mima equation can be written as follows:

$$\frac{\partial}{\partial t}(\nabla^2\phi - \lambda^2\phi) + J(\phi, \nabla^2\phi) = D + F, \quad (1)$$

where $J(a,b) = a_x b_y - a_y b_x$, $\phi(x,y)$ represents the electrostatic potential for the plasma or the variable part of the depth of the atmosphere in geostrophic flow, and D and F are damping and forcing, respectively. The parameter λ is the ratio of the system size L to the characteristic spatial scale ρ_s, the ion Larmor radius in plasma and the Rossby radius in the atmosphere. We neglect wave effects, assuming that the flow is in a strong-turbulence regime [11].

Similar to the Navier-Stokes equation, Eq. (1) has two quadratic inviscid invariants: energy, $W = W_{\text{kin}} + W_\lambda = L^{-2}\int[(\nabla\phi)^2 + \lambda^2\phi^2]dx\,dy = \sum_k (k^2 + \lambda^2)\,|\phi_k|^2$, and potential enstrophy, $U = U_f + U_\lambda = L^{-2}\int[(\nabla^2\phi)^2 + \lambda^2(\nabla\phi)^2]dx\,dy = \sum_k k^2(k^2 + \lambda^2)\,|\phi_k|^2$. Both total energy and total potential enstrophy consist of two terms which may be referred to, respectively, as kinetic energy W_{kin}, internal energy W_λ, fluid enstrophy U_f, and "internal" enstrophy U_λ. Statistical quasiequilibrium arguments [12–14] show the existence of a dual cascade similar to 2D Navier-Stokes turbulence: inverse cascade of energy W and direct cascade of potential enstrophy U.

 0031-9007/95/75(13)/2486(4)$06.00

In two limiting cases, when the spectra are concentrated at either $k \gg \lambda$ or at $k \ll \lambda$, the input of one piece of the energy ($W_{\rm kin}$ or W_λ) and the enstrophy (U_f or U_λ) dominates over the input of the other throughout most of the spectrum. Assuming the existence of an inertial range, one can obtain energy spectra from dimensional analysis. In the region where $k \gg \lambda$, $W \simeq W_{\rm kin} \gg W_\lambda$, thus leading to the well-known energy spectra for 2D Navier-Stokes turbulence: $W(k) \propto k^{-5/3}$ for the inverse and $W(k) \propto k^{-3}$ for the direct cascade [14]. In the region where $k \ll \lambda$, the total energy is dominated by internal energy, $W \simeq W_\lambda \gg W_{\rm kin}$, and one obtains $W(k) \propto k^{-11/3}$ and $W(k) \propto k^{-5}$, respectively [11,15]. Thus we can expect that in the latter case a steep energy spectrum impedes the formation of small-scale coherent vortices.

We solve Eq. (1) numerically by using hyperviscosity $D = (-1)^{p+1}\nu_p \nabla^{2p}(\nabla^2\phi), p = 8$, in order to confine dissipation to small scales. White noise, random in time and wave-number forcing F, is applied in a narrow shell Δk around k_f. The computations for various values of λ and k_f have been performed using a pseudospectral code with a square domain $L \times L$, $L = 2\pi$, periodic boundary conditions, and resolution 256×256. For intermittency diagnostics we use the potential vorticity kurtosis (flatness), defined as $\mathcal{F} = \langle \xi^4 \rangle / \langle \xi^2 \rangle^2$, and the kurtosis $F_4(r)$ of the potential vorticity increments $\xi(\mathbf{x} + \mathbf{r}) - \xi(\mathbf{x})$, where the potential vorticity is $\xi = \nabla^2\phi - \lambda^2\phi$, $\langle\rangle$ denotes an area average over $\mathbf{x} = (x, y)$, and $\mathbf{r} = r\hat{\mathbf{x}}$ or $r\hat{\mathbf{y}}$. Both $\mathcal{F}$ and $F_4(r)$ are equal to 3 for a Gaussian field, and increase when intermittency develops.

The fundamental difference between Navier-Stokes flow and solutions to the Hasegawa-Mima equations forced at $k_f > \lambda$ is that the inverse energy cascade in the latter case is shielded at $k \simeq \lambda$. As the inverse cascade transfers energy to $k \ll \lambda$, the structure of (1) becomes

$$\frac{\partial \phi}{\partial \tau} - J(\phi, \nabla^2\phi) - D - F = 0, \qquad (2)$$

where $\tau = t/\lambda^2$ is a rescaled (slower) time. This means that the energy transfer to scales larger than $\rho_s \sim \lambda^{-1}$ slows down. Freely decaying turbulence ($F = 0$) described by Eq. (2), with initial spectra concentrated at $k_0 < \lambda$, was studied in [15]. We are particularly interested in the driven-damped case when the forcing is applied at $k_f > \lambda$ (the relevant setup for the decaying case would be when the narrow initial spectra are concentrated at $k_0 > \lambda$), so that energy is transferred toward the region $k < \lambda$. In this case the flow passes through a transitional regime, when both terms, $\nabla^2\phi$ and $\lambda^2\phi$, in Eq. (1) are important. Then we expect that coherence vortex formation due to deformation radius effects will reveal itself more clearly than in the Navier-Stokes equation, when the only length scale is the box size, and these effects may well be overshadowed by the fast formation of ultraviolet vortices if no special measures are undertaken [7]. To take into account the effect of variable λ, we introduced the characteristic eddy turnover time as $\tau_\lambda(t) = U(t)^{-1/2}(1 + U_\lambda/U_f)$ (cf. Ref. [15]). We can then define a new nondimensional time N_λ, which equals the number of average eddy turnovers during the absolute time t_0: $N_\lambda = \int_0^{t_0} dt/\tau_\lambda(t)$.

Before the maximum of the energy spectra reaches the wave number $k = O(\lambda)$, there is no evidence of the appearance of coherent vortices. The values of both $\mathcal{F}$ and $F_4(r)$ remain close to their Gaussian value 3. Later, the characteristic length scale $\rho_s \sim \lambda^{-1}$ interferes with the upscale energy cascade and serves as a kind of "shield" for it. Energy starts piling up at $k = O(\lambda)$, thus promoting the formation of long-lived coherent vortices. Consequently, the number of vortices is determined by

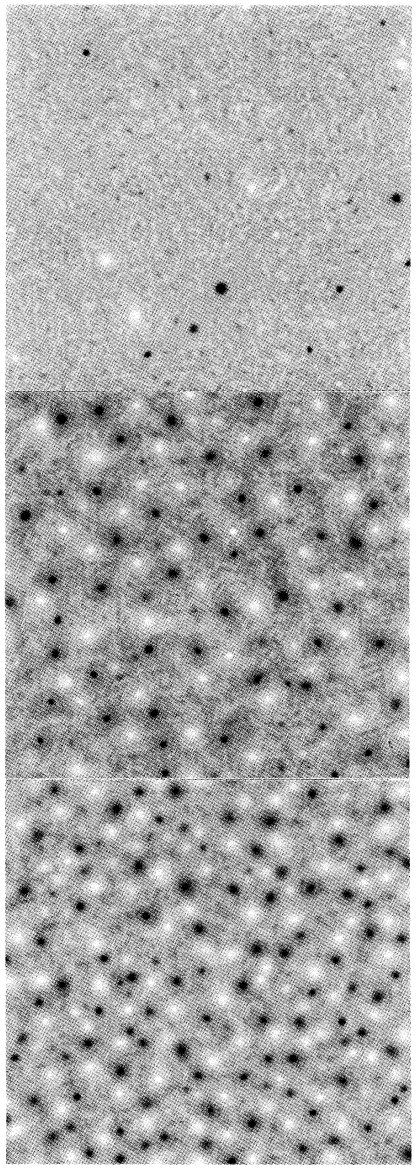

FIG. 1. The potential vorticity, $\xi = \nabla^2\phi - \lambda^2\phi$, field at $N_\lambda = 400$ for the NS and the HM equations: (a) $\lambda = 0$ (NS), (b) $\lambda = 20$, and (c) $\lambda = 40$.

the ratio $\lambda = L/\rho_s$. This is illustrated in Fig. 1, where we plot the instantaneous potential vorticity fields at the same nondimensional time $N_\lambda = 400$ (this corresponds to about $120\tau_0$, where $\tau_0 \sim \pi/v_{\rm rms}$ is a large-eddy turnover time) for the cases with forcing at $47 < k_f < 50$ and $\lambda = 0$ (NS), $\lambda = 20$, $\lambda = 40$. The values of absolute time t and kurtosis $\mathcal{F}$ at that time were $t \simeq 65$, $\mathcal{F} = 21$ ($\lambda = 0$); $t \simeq 100$, $\mathcal{F} = 10.5$ ($\lambda = 20$); $t \simeq 210$, $\mathcal{F} = 6.5$ ($\lambda = 40$).

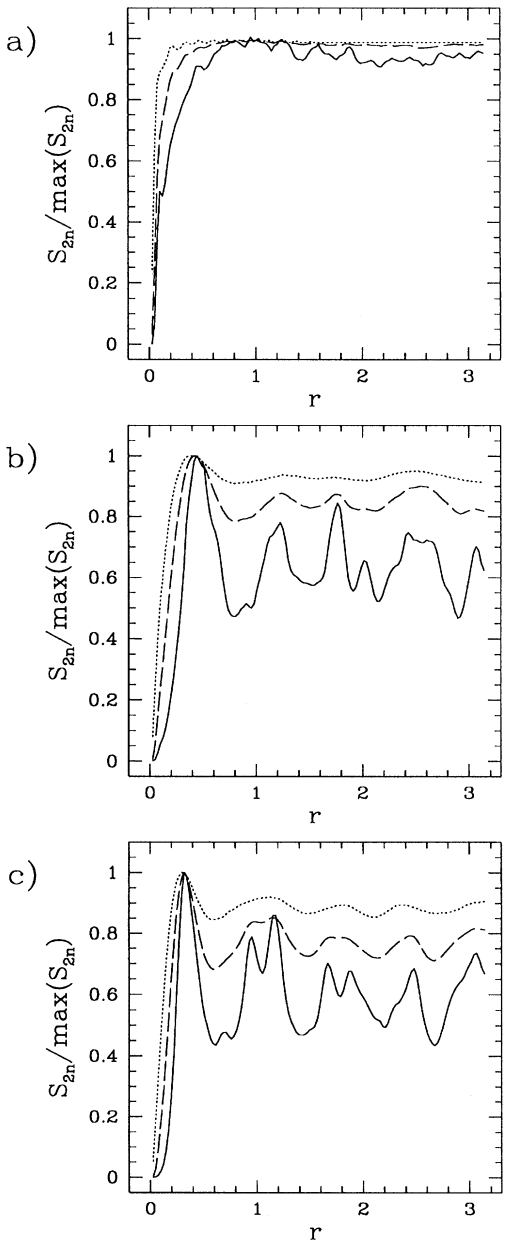

FIG. 2. Moments of potential vorticity increments $S_2(r)$ (dotted), $S_4(r)$ (dashed), and $S_8(r)$ (solid) normalized to their maximum values and averaged over time $N_\lambda \in [0, 400]$ for (a) $\lambda = 0$ (NS); (b) $\lambda = 20$, $\rho_s \simeq 0.32$; and (c) $\lambda = 40$, $\rho_s \simeq 0.16$.

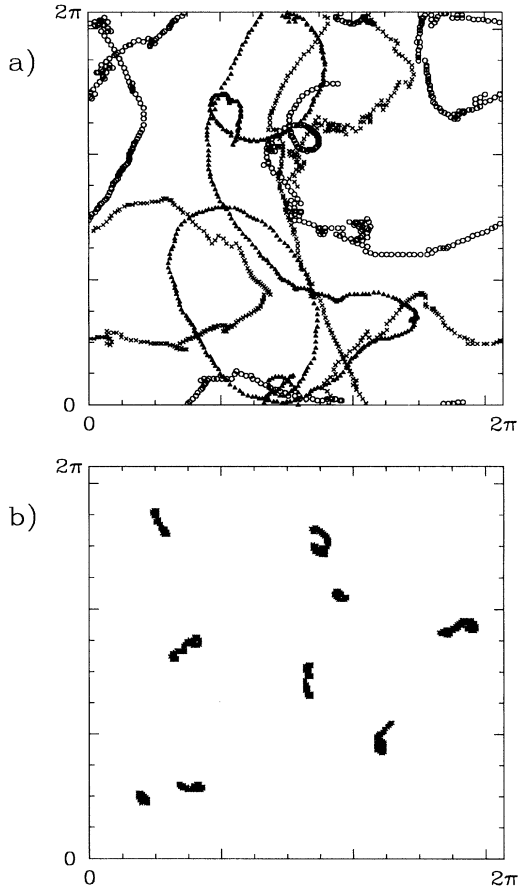

FIG. 3. Trajectories of several vortices during $\Delta N_\lambda = 170$ for (a) the NS equation (three vortices), $t \in [100, 125]$, and (b) the HM equation (nine vortices), $\lambda = 40$, $t \in [100, 200]$.

The remarkable fact is that although the spectra shield is permeable (i.e., energy transfer to $k < \lambda$ does not vanish), one can detect the appearance of order, i.e., in some sense the formation of a "liquid" or even a quasicrystal of vortices. For this purpose we consider the space-time averaged even-order moments of potential vorticity increments (structure functions),

$$S_{2n}(r) = \langle [\xi(\mathbf{x} + \mathbf{r}) - \xi(\mathbf{x})]^{2n} \rangle . \tag{3}$$

The results for $S_{2n}(r)$ demonstrate the presence of long-range order, characteristic of the quasicrystalline phase. The moments $S_2(r)$, $S_4(r)$, and $S_8(r)$, averaged over the same interval of time $N_\lambda \in [0, 400]$ for the Navier-Stokes equation ($\lambda = 0$) and the Hasegawa-Mima equation with $\lambda = 20$ and $\lambda = 40$, are plotted in Fig. 2. The value of $S_{2n}(r)$ is practically constant for the Navier-Stokes equation [Fig. 2(a)], while for the Hasegawa-Mima equation one can easily distinguish periodical oscillations. The first peak of $S_{2n}(r)$ with maxima at r slightly larger than ρ_s [Figs. 2(b) and 2(c)] denotes a shell of nearest vortex neighbors, and there are oscillations representing more distant neighbors. We emphasize that the observed vortical structure looks like a quasicrystal, rather than liquid

or dense gas [16]. In liquids the form factors (structure functions) exhibit a few oscillations with a period r_0 (corresponding to the scale of interatomic potential), rapidly decaying at $r > r_0$. As one can see from Figs. 2(b) and 2(c), no such decay is observed in our simulations, leading to the conclusion that the vortices form a quasicrystal. Although the inverse energy cascade to $k < \lambda$ is suppressed, it still exists, so vortices continue to coalesce. As a result, the mean period of the quasilattice increases with time. However, in contrast to their counterparts in Navier-Stokes turbulence, the vortices resulting from Eq. (1) are screened since the velocity field from a given vortex ξ exponentially decays on a scale λ^{-1} [15]. Consequently, the vortices just oscillate on the order of the characteristic length scale, so that the latticelike structure maintains for a long time. The trajectories of several vortices for the Hasegawa-Mima and the Navier-Stokes equations during the same interval of time, $\Delta N_\lambda = 170$, are plotted in Fig. 3.

We observe gradual steepening of the energy spectrum as λ increases while k_f is kept the same. Time-averaged energy spectra for $47 < k_f < 50$ and $\lambda = 10, 20, 40$ are plotted in Fig. 4. The results are well suited to the expectation that the energy spectrum should steepen from $-5/3$ for pure Navier-Stokes turbulence (when $k \gg \lambda$) to $-11/3$ for the asymptotic case $k \ll \lambda$. Knowledge of these spectral exponents can be used as a starting point for understanding the reasons for the appearance of the long-range order discovered here. It is easy to show that the renormalized perturbation expansion, based on the spectra evaluated above, is infrared divergent; i.e., each term depends on the infrared cutoff. It is possible that the large correlation length, created as a result of vortex crystallization, is a dynamic manifestation of the nontrivial infrared properties of the system and is analogous to the condensate state proposed by Polyakov in his conformal theory of 2D turbulence [17]. In the case considered here,

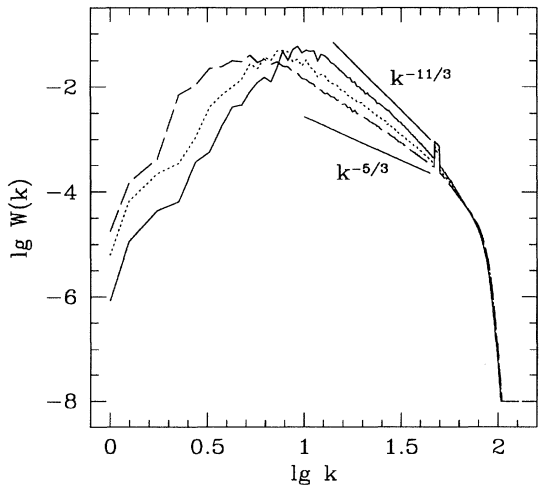

FIG. 4. Time-averaged ($N_\lambda \in [0, 500]$) energy spectra for $47 < k_f < 50$: $\lambda = 10$ (dashed), $\lambda = 20$ (dotted), and $\lambda = 40$ (solid).

crystallization is a natural dynamic mechanism due to the existence of a screening length $\rho_s \sim \lambda^{-1}$. The effect of the long-range order on the scaling exponents of the energy spectra is an interesting subject which is beyond the scope of this paper. Finally, we would like to note that when $k_f \ll \lambda$ coherent vortices, once they emerge, also reveal a quasicrystalline structure. Detailed studies of this issue will be given in a later paper.

To conclude, we have shown that the presence of a characteristic spatial scale in the Hasegawa-Mima equation leads to the formation of coherent vortices. The steeper inertial range energy spectra, in comparison with Navier-Stokes turbulence (up to $-11/3$ and -5 for inverse and direct cascades, respectively), result in a smaller influence of ultraviolet vortices on the formation of coherent structures. In a transitional regime, when the energy is transferred from $k > \lambda$ to $k < \lambda$, the spectrum $W(k)$ indicates energy accumulation at $k = O(\lambda)$ as a result of spectral "shielding." This leads to the formation of coherent vortices due to finite-size effects. These vortices are less isolated and less movable in comparison with their counterparts in Navier-Stokes turbulence. The calculation of moments of the potential vorticity increments shows the appearance of the long-range order in the medium, indicating the formation of a vortical quasicrystal.

We would like to thank V. Borue for useful discussions. This work was supported by ONR/ARPA under Grant No. N00014-92-J-1796 and by DOE under Grant No. DE-FG02-93ER54204.

[1] J. C. McWilliams, J. Fluid Mech. **146**, 21 (1984).
[2] M. Brachet, M. Meneguzzi, H. Politano, and P. Sulem, J. Fluid Mech. **194**, 333 (1988).
[3] B. Legras, P. Santangelo, and R. Benzi, Europhys. Lett. **5**, 37 (1988).
[4] W. H. Matthaeus, W. T. Stribling, D. Martinez, S. Oughton, and D. Montgomery, Physica (Amsterdam) **51D**, 531 (1991).
[5] N. N. Kukharkin, J. Sci. Comput. (to be published).
[6] L. M. Smith and V. Yakhot, Phys. Rev. Lett. **71**, 352 (1993).
[7] L. M. Smith and V. Yakhot, J. Fluid Mech. **274**, 115 (1994).
[8] A. Hasegawa and K. Mima, Phys. Fluids **21**, 87 (1978).
[9] M. V. Nezlin and E. N. Snezhkin, *Rossby Vortices, Spiral Structures, Solitons* (Springer-Verlag, Berlin, 1993).
[10] W. Horton and A. Hasegawa, Chaos **4**, 227 (1994).
[11] M. Ottaviani and J. Krommes, Phys. Rev. Lett. **69**, 2923 (1992).
[12] R. H. Kraichnan, Phys. Fluids **10**, 1417 (1967).
[13] D. Fyfe and D. Montgomery, J. Plasma Phys. **17**, 317 (1977).
[14] D. Fyfe and D. Montgomery, Phys. Fluids A **3**, 938 (1991).
[15] V. D. Larichev and J. C. McWilliams, Phys. Fluids A **3**, 938 (1991).
[16] J. D. Weiss and W. Horton, Phys. Rev. Lett. **48**, 1362 (1982).
[17] A. Polyakov, Nucl. Phys. **B396**, 367 (1993).

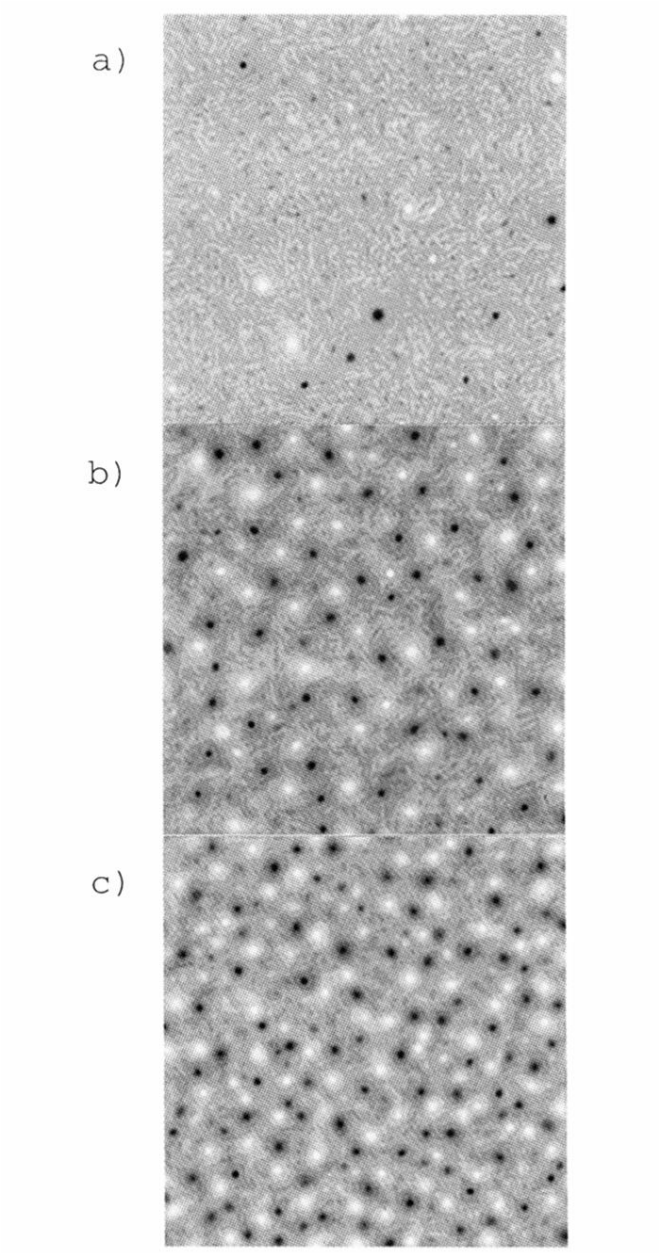

FIG. 1. The potential vorticity, $\xi = \nabla^2\phi - \lambda^2\phi$, field at $N_\lambda = 400$ for the NS and the HM equations: (a) $\lambda = 0$ (NS), (b) $\lambda = 20$, and (c) $\lambda = 40$.